Surface level migration in vibrating beds of cohesionless granular materials

Toshiya Ohtsuki
Faculty of Science, Yokohama City University, Kanazawa-ku, Yokohama 236, Japan

Daisuke Kinoshita, Yasushi Nakada, and Akihisa Hayashi
Department of Applied Physics, Fukui University, Fukui 910, Japan

(Received 3 February 1998)

Surface level migration in vibrating beds of cohesionless granular materials is investigated experimentally, numerically, and theoretically. The difference in surface levels of narrow and wide regions is measured for various values of the vessel size, particle size, and frequency and power of vibration. The effects of these parameters on surface level migration are clarified. A molecular dynamics technique is used to calculate various physical quantities, especially, wall shear stresses. It becomes evident that side walls exert downward forces on particles and the friction between particles and walls play an essential role in surface level migration. A vertical force balance on a layer of the material is analyzed and a formula for the difference of surface levels is derived. The theoretical results are compared with numerical ones. The theory and the simulation agree qualitatively. [S1063-651X(98)09312-X]

PACS number(s): 81.05.Rm, 05.40.+j, 47.20.Ky, 83.10.Pp

I. INTRODUCTION

Since the pioneering work by Faraday [1], vibrating beds of cohesionless granular materials have attracted considerable attention of many researchers not only in powder technology but also in physics (See, e.g., Refs. [2] and [3]). They exhibit a wide variety of dynamical behaviors such as heaping [4], convection [5], segregation [6], bubbling [7], and surface waves [8]. Recently, Akiyama and Shimomura [9,10] have reported a novel phenomenon: When a tube is immersed in a vibrating bed and held stationary, the surface level of particles within the tube becomes different from that outside. We refer to this phenomenon as ''surface level migration.'' The difference in surface levels depends on a number of parameters such as particle size, frequency and amplitude of vibration, height of beds, and difference in area of two regions [11]. Usually, the surface in the narrow region in the tube falls. In some cases, however, the surface level of a narrow region becomes higher than that of a wide region and even a bistable state appears [12]. Apparently, surface level migration is similar to capillary phenomena. It is well known that capillarity of ordinary liquids comes from surface tension. In contrast, little is known about the mechanism of surface level migration of granular materials. The purpose of this paper is to investigate surface level migration in vibrating powder beds experimentally, numerically, and theoretically and to make progress in the understanding of the phenomenon.

In Sec. II, we perform experimental studies and measure effects of the vessel size, particle size, and frequency and power of vibration. In Sec. III, a molecular dynamics technique is used to simulate numerically and various physical quantities, particularly, wall shear stresses, are calculated. Section IV is devoted to theoretical explanation based upon numerical data obtained in Sec. III. Finally in Sec. V, we summarize and discuss our results.

II. EXPERIMENT

We used an acrylic vessel of width L and thickness $b = 2.4$ cm, shown in Fig. 1. It has a partition of thickness $l_0 = 0.2$ cm which divides the vessel into two regions of width l_1 and $l_2 = L - l_0 - l_1$. The partition is attached $d = 1.0$ cm away from the bottom of the vessel and two regions are interconnected through a gap of thickness d. In order to investigate effects of vessel width, we prepared several sizes of vessels with $L = 3.2$–6.2 cm and $l_1 = 0.6$–1.8 cm. As for granular particles, we used three size ranges of glass beads of diameter $r = 0.018$–$0.025(0.02)$ cm, 0.050–$0.071(0.06)$ cm, and 0.099–$0.140(0.10)$ cm. Hereafter we represent them by typical values shown in parentheses. The vessel is vibrated by a speaker where a frequency f and an applied voltage V are controlled. The form of the waves was checked by an oscilloscope and found to be sinusoidal. The frequency f is varied in a range from 10 to 100 Hz and the voltage V is

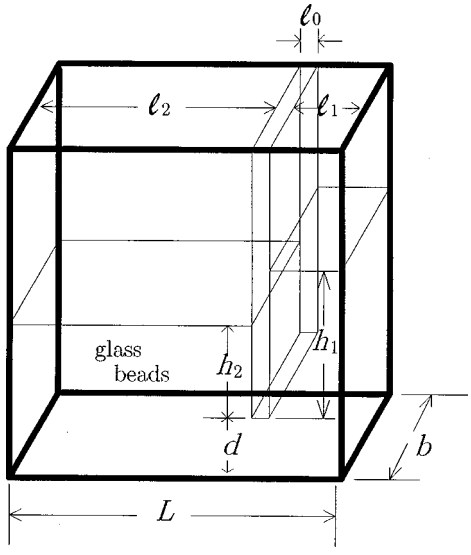

FIG. 1. Schematic diagram of a vessel.

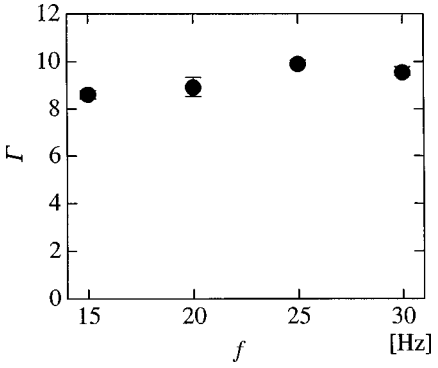

FIG. 2. Frequency dependence of the ratio Γ of the vibratory to gravity acceleration ($V=30$ V).

changed from 10 to 30 V. The ratio $\Gamma \equiv A(2\pi f)^2/g$ of the vibratory to gravity acceleration was calculated from measured values of the vibration amplitude A. Figure 2 shows results at $V=30$ V and $f=15-30$ Hz. The ratio Γ turned out to be almost constant. After vibration of several minutes, the system reached a steady state independent of initial conditions. Then the height h_1 of the surface of the particle bed in a narrow region of width l_1 and that h_2 in a wide region of width l_2 were measured. The zero point of height was assigned at the bottom of the partition. Note that the surface of the vibrating bed is generally inclined. In the present work, h_1 and h_2 stand for average values of the highest and the lowest points of the surface. The experiment was performed several times under different circumstances such as the di-

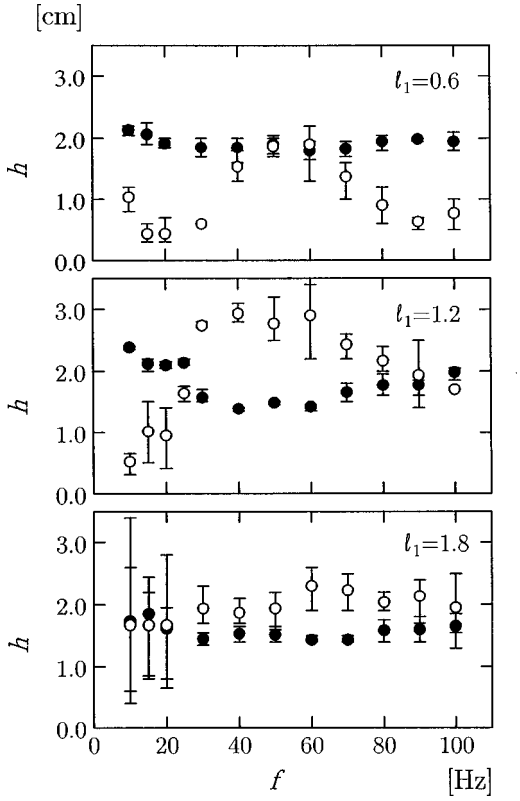

FIG. 4. Effects of the vessel size on heights h of particle beds at constant width $L=6.2$ cm in narrow (○) and wide (●) regions ($V=30$ V, $r=0.06$ cm).

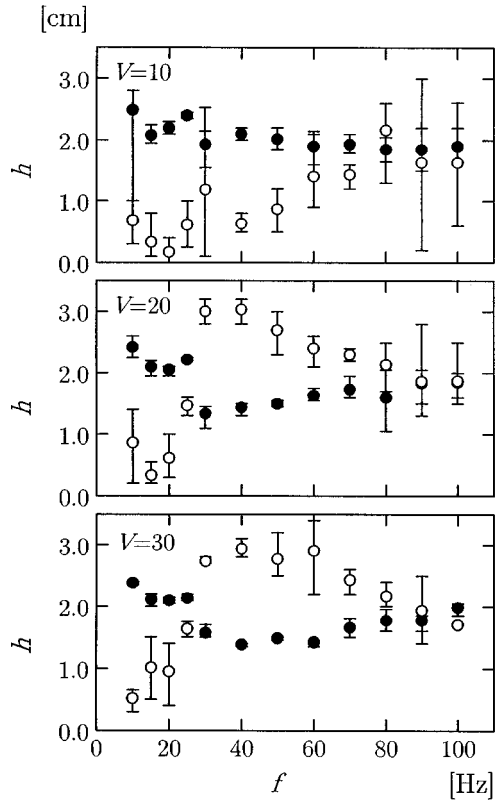

FIG. 3. Effects of the applied voltages on heights h of particle beds in narrow (○) and wide (●) regions ($l_1=1.2$ cm, $L=6.2$ cm, $r=0.06$ cm).

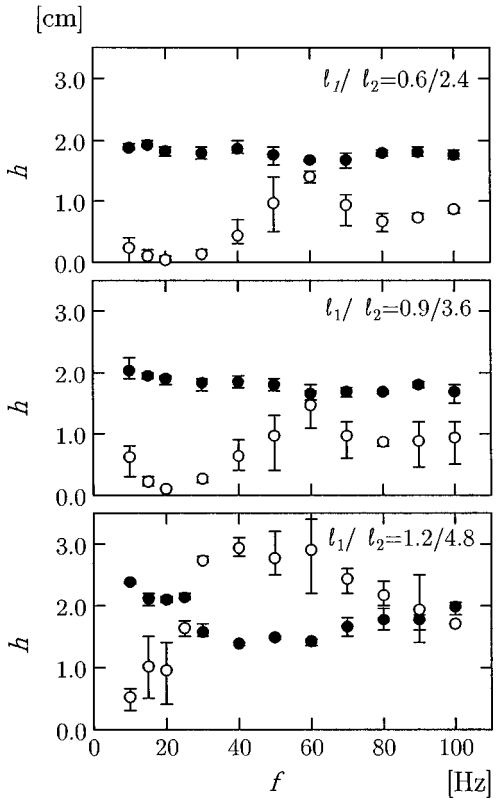

FIG. 5. Effects of the vessel size on heights h of particle beds at constant ratio $l_1/l_2=\frac{1}{4}$ in narrow (○) and wide (●) regions ($V=30$ V, $r=0.06$ cm).

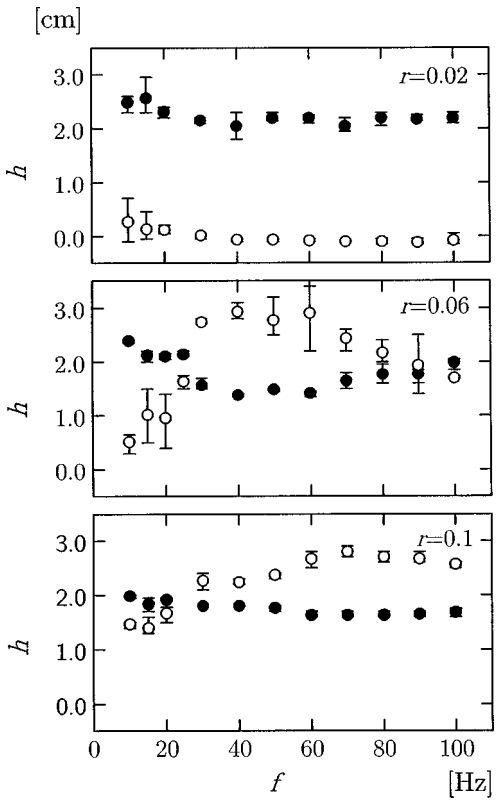

FIG. 6. Effects of the particle size on heights h of particle beds in narrow (○) and wide (●) regions ($l_1=1.2$ cm, $L=6.2$ cm, $V=30$ V).

rection of frequency change (increase or decrease), the location of the narrow region (left side or right side), and the time and date.

The results are shown in Figs. 3–6. Here heights of particle beds are plotted as a function of the frequency f of vibration. Heights h_1 in a narrow region are denoted by open circles and those h_2 in a wide region are indicated by solid circles. In Fig. 3, heights for values of $V=10-30$ V are plotted, which shows that the qualitative features are independent of V. At low frequencies, the surface level h_1 of the narrow region is much lower than that of the wide region h_2. With increasing frequency, h_1 rises and exceeds h_2. In the high frequency region, h_1 and h_2 are almost equal and other dynamical behaviors such as convection was not observed. It

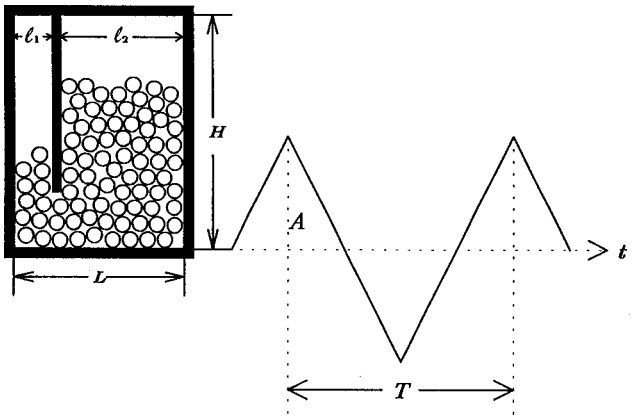

FIG. 7. Schematic diagram of simulations.

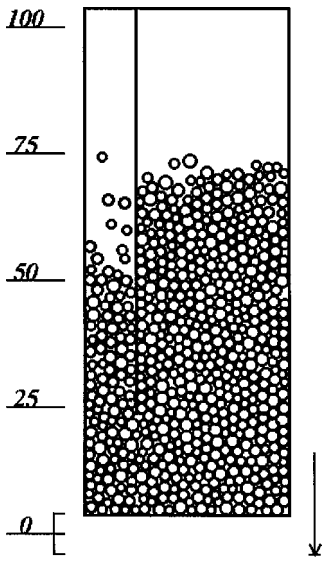

FIG. 8. Snapshot of simulations ($\mu_w=0.5$, $A=4.0$, $T=2.0$, $N=600$).

is considered that in this region, the estimated amplitude of vibration is much less than the bead size and the particle bed is inactive. In the next two figures, effects of the vessel size are examined. In Fig. 4, the width L of the whole vessel is kept constant at 6.2 cm and the width l_1 of a narrow region is changed, whereas in Fig. 5, the ratio l_1/l_2 is fixed at $\frac{1}{4}$ and L is altered. At $l_1=1.8$ cm, h_1 is nearly equal to h_2 at all frequencies. When $l_1 \lesssim 1.0$ cm, on the contrary, h_1 is much lower than h_2 and surface level migration clearly takes place. In addition, frequency dependence in these three cases is similar. It should be noted that in Fig. 5 where the vessel size is changed keeping the similarity, the upper two results are almost the same but the bottom one is qualitatively different. The coexistence of similar and nonsimilar behaviors suggests that a simple scaling relation does not hold. Rather, the absolute value of l_1 seems to play an important role in surface level migration. In Fig. 6, results of three size ranges of glass beads are compared. We find that the particle size exerts an important influence on surface level migration. In the case $r=0.02$ cm, the surface level of the narrow region always

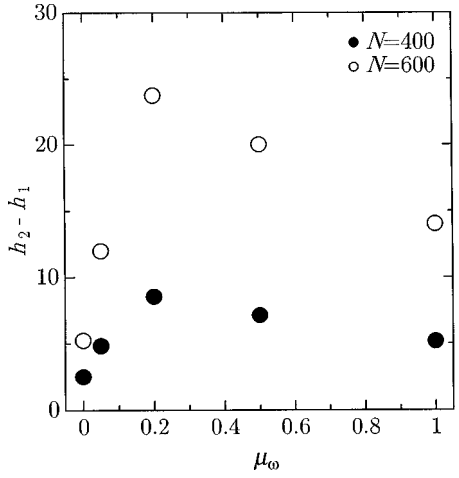

FIG. 9. Difference of heights h_2-h_1 as a function of the particle-wall friction coefficient μ_w ($A=4.0$, $T=2.0$).

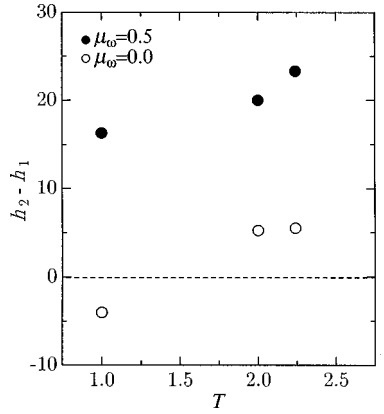

FIG. 10. Period dependence of the difference of heights $h_2 - h_1$ ($\Gamma = 39.4$, $N = 600$).

falls, while at $r = 0.10$ cm, h_1 exceeds h_2 except at low frequencies. At an intermediate size $r = 0.06$ cm, h_1 varies rapidly with changing the frequency f.

III. SIMULATION

Simulations were carried out for two-dimensional systems where granular particles are modeled by inelastic hard disks with both translational and rotational degrees of freedom [13]. The simulation is schematically illustrated in Fig. 7. N particles of radius r and mass m are confined to a rectangular box with a partition of zero thickness. The box oscillates with a triangular wave form of period T and amplitude A. Interparticle collisions are assumed to be the standard center-of-mass hard-core collisions. The precollision and postcollision relative particle velocities $\mathbf{v}_\perp$ normal to the surface at contact are related by

$$\mathbf{v}_\perp' = -e_p \mathbf{v}_\perp , \tag{1}$$

where e_p is a coefficient of restitution and the prime denotes a postcollisional quantity. The force $\mathbf{f}_\parallel$ acting tangential to the surface is subject to Coulomb's law

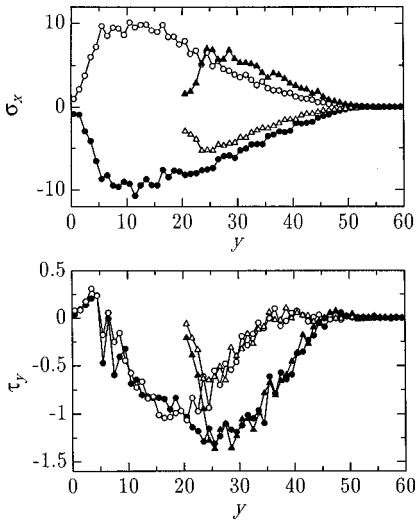

FIG. 11. Normal σ_x and shear τ_y stresses exerted by side walls on particles at $\mu_w = 0.5$ ($A = 4.0$, $T = 2.0$, $N = 400$).

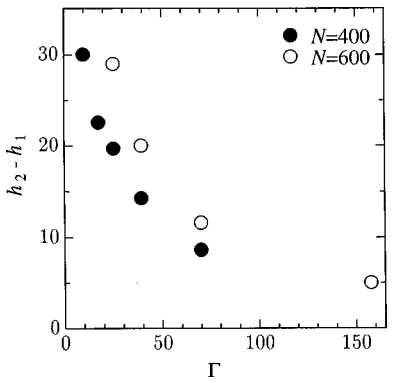

FIG. 12. Effects of the ratio Γ of the vibratory to gravity acceleration on the height difference $h_2 - h_1$ ($\mu_w = 0.5$, $A = 4.0$).

$$\mathbf{f}_\parallel' = -\mu_p |\mathbf{f}_\perp| \frac{\mathbf{v}_\parallel}{|\mathbf{v}_\parallel|}, \tag{2}$$

where μ_p is a friction coefficient, $\mathbf{f}_\perp$ is the normal force, and $\mathbf{v}_\parallel$ is the relative velocity tangential to the surface. When the friction force obtained from Eq. (2) is large enough to change the sign of $\mathbf{v}_\parallel$, the so-called fully rough surface condition

$$\mathbf{v}_\parallel' = \mathbf{0}, \tag{3}$$

is used in place of Eq. (2). Translational and angular velocities of particles after collision are completely determined from Eqs. (1), (2), or (3), and conservation laws of translational and angular momentum. Collision between a particle and a solid wall is similarly defined with a coefficient of restitution e_w and a friction coefficient μ_w. Initially particles are arranged in a square lattice and particle velocities are chosen to be random. Note that initial conditions are irrelevant to steady state properties. In the present simulations, we chose units of length, mass, and time such that $\langle r \rangle = \langle m \rangle = g = 1$, where g is the gravity acceleration and the brackets denote the average. The radius r and mass m of particles are uniformly distributed in a range $r = 0.8 \sim 1.2$ and

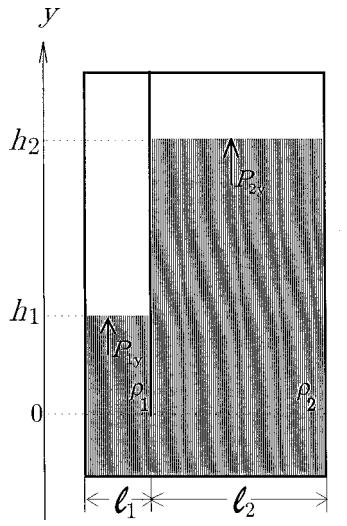

FIG. 13. Schematic diagram of boundary conditions for pressures P_{1y}, P_{2y} in a vessel with a partition.

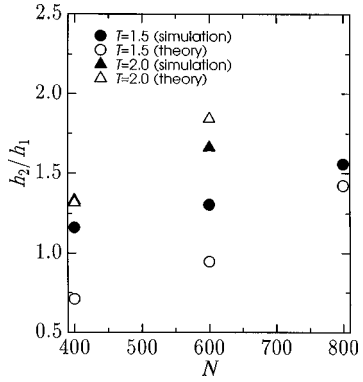

FIG. 14. Comparison of the theory and the simulation for the ratio of heights h_2/h_1 ($\mu_w=0.5$, $A=4.0$).

$m=0.64\sim1.44$, which corresponds approximately to experimental conditions. The number N of particles is changed from 400 to 800. The vessel size is given by $L=40.0$, $l_1=10.0$, $l_2=30.0$, $d=20.0$, and $H=100.0-150.0$. The period T and amplitude A of oscillation are chosen such that $T=0.5-3.0$ and $A=0.25-9.0$. Notice that $\Gamma\equiv A(2\pi/T)^2/g$ is in most cases much larger than unity and the system is highly accelerated. Later we will see that the friction between particles and side walls exerts a strong influence. Among the various coefficients of restitution and friction, therefore, μ_w is widely varied from 0.0 to 1.0, while the other parameters are fixed at $e_p=e_w=0.95$ and $\mu_p=0.2$.

Figure 8 shows a snapshot of simulations at $\mu_w=0.5$. The surface of a wide region rises substantially and surface level migration takes place. In the absence of friction $\mu_w=0.0$, on the other hand, the difference in surface levels are quite small. In order to treat quantitatively, we have calculated heights h_1 and h_2 of surface levels in narrow and wide regions at steady states. Here h_i is defined by $h_i=4n_i/l_i(i=1,2)$, where n_i is a number of particles in each region. In Fig. 9, μ_w-dependence of the difference of heights h_2-h_1 is plotted. With increasing μ_w, h_2-h_1 increases rapidly and then decreases gradually. The influence of the frequency of oscillation is checked in Fig. 10. Here h_2-h_1 is plotted as a function of T, where Γ is kept constant. At all periods, h_2-h_1 at $\mu_w=0.0$ is almost zero, whereas that of $\mu_w=0.5$ is always large. It becomes evident that the friction between particles and side walls play an essential role in surface level migration. Thus, we have computed wall shear stresses. Figure 11 shows normal and shear stresses σ_x, τ_y exerted by side walls on particles as a function of vertical position y from the bottom of the vessel. Here circular, triangular, open, and solid symbols represent stresses by outer walls, by inner walls, in a narrow region, and in a wide region, respectively. Stresses in a wide region are larger than those in a narrow region. In addition, $\tau_y<0$, that is, side walls exert downward shear stresses. It is well known that in static powder beds, the direction of wall shear stress is upward such that the side walls support the particles. It should be emphasized that when subject to the vibration, wall shear stresses act in the opposite direction to those in static beds, and the side walls push particles down. Figure 12 shows the acceleration (Γ) dependence of h_2-h_1, where amplitude A is fixed at 4 and period T is varied from 4 to 1. We find that h_2-h_1 is a monotonically decreasing function of Γ and surface level migration is suppressed at high Γ.

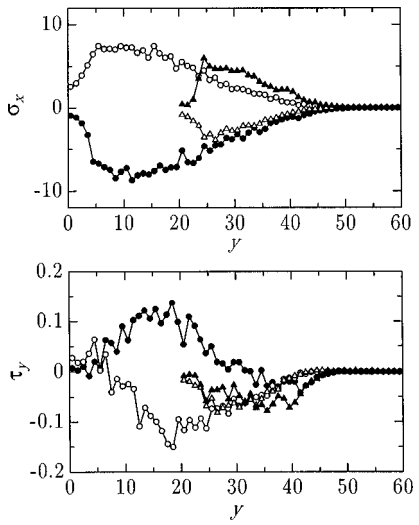

FIG. 15. Normal σ_x and shear τ_y stresses exerted by side walls on particles at $\mu_w=0.05$ ($A=4.0$, $T=3.0$, $N=400$).

IV. THEORY

In static powder beds, Janssen [14] employed a simple force balance on elemental slices and derived a well-known formula for the stress distribution [15]. In this section, we perform a similar analysis for vibrating beds based upon the following two assumptions: (i) Stresses are uniform across any horizontal section of the material and (ii) wall shear stresses are proportional to horizontal stresses and the proportional coefficient is independent of the height of the system. The forces supported by a layer at height $y\sim y+dy$ are composed of stresses from adjacent layers, those from side walls, and gravity. A dynamical version of Janssen's treatment has been reported in Ref. [16]. In the present paper, however, we consider only steady states and neglect inertia terms. The resulting vertical force balance in a two-dimensional system reads

$$\int_0^L \{P_y(x,y)-P_y(x,y+dy)\}dx+2\tau_y dy-\int_0^L \rho g dy dx=0, \tag{4}$$

where P_y is the vertical compressive stress and ρ is the density of the material. Simulations show that in vibrating beds of $\Gamma>1$, particles behave similar to molecules in normal gases and the stress is locally isotropic:

$$P_x(x,y)=P_y(x,y). \tag{5}$$

Assumption (ii) leads to

$$\tau_y=-\mu^* P_x, \tag{6}$$

where $\mu^*>0$ is an effective wall friction coefficient. The negative sign reflects the fact that τ_y is downward. Substitution of Eqs. (5) and (6) into Eq. (4) together with assumption (i) yields

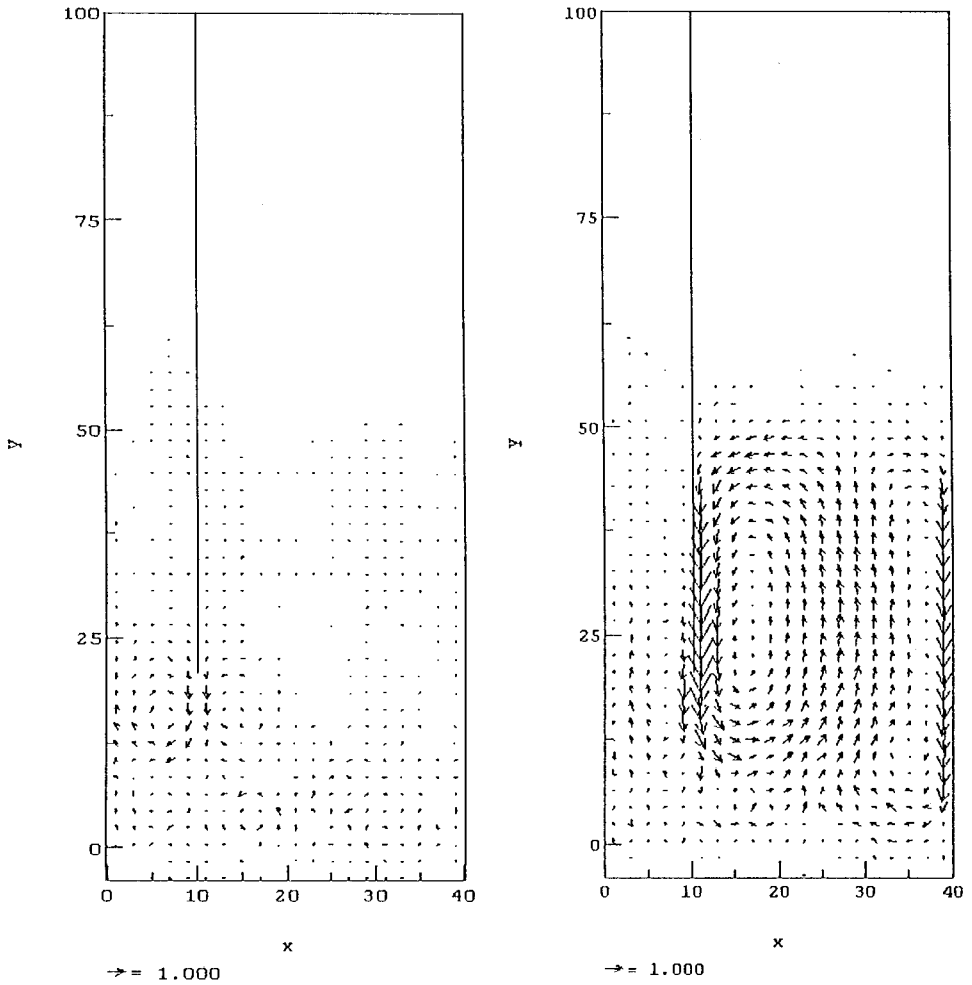

FIG. 16. Vector plot of momentum flux in the presence ($\mu_w = 0.5$) and in the absence ($\mu_w = 0.0$) of the particle-wall friction ($A = 4.0$, $T = 2.0$, $N = 400$).

$$\mu_w = 0.0$$

$$-\frac{dP_y}{dy} - \frac{2\mu^*}{L} P_y - \rho g = 0 \tag{7}$$

and then

$$P_y(y) = C \exp\left(-\frac{2\mu^*}{L} y \right) - \frac{\rho g L}{2\mu^*}, \tag{8}$$

where C is an integration constant.

Now we consider a force balance in a system with a partition illustrated in Fig. 13. Equation (8) holds for pressures P_{1y} and P_{2y} in each region. At the free surfaces, pressures are zero

$$P_{1y}(h_1) = 0, \tag{9}$$

$$P_{2y}(h_2) = 0, \tag{10}$$

and at the end of the partition, both pressures are equated:

$$P_{1y}(0) = P_{2y}(0). \tag{11}$$

The boundary conditions (9) and (10) determine integration constants and the condition (11) together with Eq. (8) gives rise to

$$\mu_w = 0.5$$

$$\frac{\rho_1 l_1}{\mu_1^*} \left\{ \exp\left(\frac{2\mu_1^*}{l_1} h_1 \right) - 1 \right\} = \frac{\rho_2 l_2}{\mu_2^*} \left\{ \exp\left(\frac{2\mu_2^*}{l_2} h_2 \right) - 1 \right\}, \tag{12}$$

where subscripts 1 and 2 represent quantities in each region. The difference $h_2 - h_1$ in the surface height in each region is decided by this relation. It should be noticed that when $\mu^* > 0$ and wall shear stresses act downward, the height in a wide region is larger than that in a narrow region. In the low and high height limit, or equivalently in the low and high friction limit, we get

$$h \to 0 (\mu^* \to 0) \cdots \rho_1 h_1 = \rho_2 h_2, \tag{13}$$

$$h \to \infty (\mu^* \to \infty) \cdots \frac{\mu_1^* h_1}{l_1} = \frac{\mu_2^* h_2}{l_2}. \tag{14}$$

When the bed height or the particle-wall friction is sufficiently large, the height of the surface level is in proportion to the width of the region.

We compare the theoretical prediction with numerical simulations in Fig. 14. Here we put $\rho_1 = \rho_2$. As for μ_1^* and μ_2^*, we adopted calculated values. We find that the theory agrees qualitatively with the simulation.

V. SUMMARY AND DISCUSSION

In this work, we have carried out experimental, numerical and theoretical studies on surface level migration in vibrating beds of cohesionless granular materials. The existence of surface level migration has been confirmed in all three ways. The effects of a number of parameters have been examined and elucidated. Roughly speaking, the factors which lead to lowering of the surface level of a narrow region and enhance surface level migration are summarized by (1) low frequencies (E), (2) low accelerations (E,S), (3) large differences in chamber widths (E,T), (4) small particles (E), (5) large bed heights (S,T), and (6) large wall friction (S,T). Here E, S, and T in parentheses denote deductions from experiment, simulation, and theory, respectively. Friction between particles and side walls turned out to play a particularly key role.

Wall shear stresses in vibrating beds are generally downward. We can present a simple explanation of this phenomenon. In one cycle of vibration, wall shear stresses act upward when the system rises. In this situation, particles are lifted by the bottom wall and the material and the vessel go up together as if they were one body. Hence wall shear stresses are relatively small. When the system descends, on the contrary, particles are left above and large downward stresses are exerted by side walls. It follows that average wall shear stresses over one cycle are downward.

In the theoretical treatment, we have assumed Eq. (6) to account for the surface level migration. On the other hand, experiments and simulations tell us that various other parameters exert strong influence on surface level migration. In other words, the coefficient μ^* and its sign, depend strongly on these parameters. Moreover, the system exhibits complex behavior. For instance, we have found an intermediate state of wall shear stress. Numerical simulations of normal and shear stresses σ_x, τ_y at $\mu_w = 0.05$ are plotted in Fig. 15. Here the shear stress on the outer wall in a wide region is upward and those on the other walls are downward. Thus, it remains to clarify a mechanism which controls wall shear stresses. Convection is one candidate [11]. Observation of both experiments and simulation, seems to suggest that downward flow along the partition plays an important role. Figure 16 shows vector plots of average momentum flux. When $\mu_w = 0.5$ and surface level migration takes place, strong convection is observed, whereas in the absence of wall friction, $\mu_w = 0.0$, and surface level migration, convective motion is also absent. However, further investigation is necessary for definite conclusions. Finally, we add a comment on interstitial pressure effects. For small particles ($r = 0.02$ cm), the pressure variations in the interstitial air has been reported to play an important role [17]. For larger particles, in contrast, little influence has been observed [17] and we believe that the qualitative nature of the phenomenon can be explained without considering the interstitial pressure.

[1] M. Faraday, Proc. R. Soc. London **52**, 299 (1831).
[2] A. Mehta and G. C. Barker, Rep. Prog. Phys. **57**, 383 (1994).
[3] H. M. Jaeger, S. R. Nagel, and R. P. Behringer, Rev. Mod. Phys. **68**, 1259 (1996).
[4] P. Evesque and J. Rajchenbach, Phys. Rev. Lett. **62**, 44 (1989).
[5] K. M. Aoki, T. Akiyama, Y. Maki, and T. Watanabe, Phys. Rev. E **54**, 874 (1996).
[6] J. L. Olsen and E. G. Rippie, J. Pharm. Sci. **53**, 147 (1964).
[7] H. K. Pak and P. R. Behringer, Nature (London) **371**, 231 (1994).
[8] F. Melo, P. Umbanhowar, and H. L. Swinney, Phys. Rev. Lett. **72**, 172 (1994).
[9] T. Akiyama and T. Shimomura, Powder Technol. **66**, 243 (1991).
[10] T. Akiyama and T. Shimomura, Adv. Powder Technol. **4**, 129 (1993).
[11] Y. Maeno, Physica A **232**, 27 (1996).
[12] H. Nishimori, Y. Tsuruta, and T. Sasaki (unpublished).
[13] C. S. Campbell and C. E. Brennen, J. Fluid Mech. **151**, 167–188 (1985).
[14] H. A. Janssen, Z. Ver. Dt. Ing. **39**, 1045 (1895).
[15] R. M. Nedderman, *Statics and Kinematics of Granular Materials* (Cambridge University Press, London, 1992).
[16] T. Boutreux, E. Raphael, and P. G. de Gennes, Phys. Rev. E **55**, 5759 (1997).
[17] T. Akiyama (private communications).